

Electronic Supplementary Information

Turbulent pattern in the 1,4-cyclohexanedione Belousov-Zhabotinsky reaction

Suparinthon Anupong,^a Igor Schreiber^b and On-Uma Kheowan^{a*}

^aDepartment of Chemistry, Faculty of Science, Mahidol University, Rama 6 Road, Bangkok 10400, Thailand. *Corresponding author e-mail: onuma.khe@mahidol.ac.th

^bDepartment of Chemical Engineering, University of Chemistry and Technology, Prague, Technicka 5, 166 28, Prague 6, Czech Republic.

ESI 1: Schematic diagram of the reaction chamber

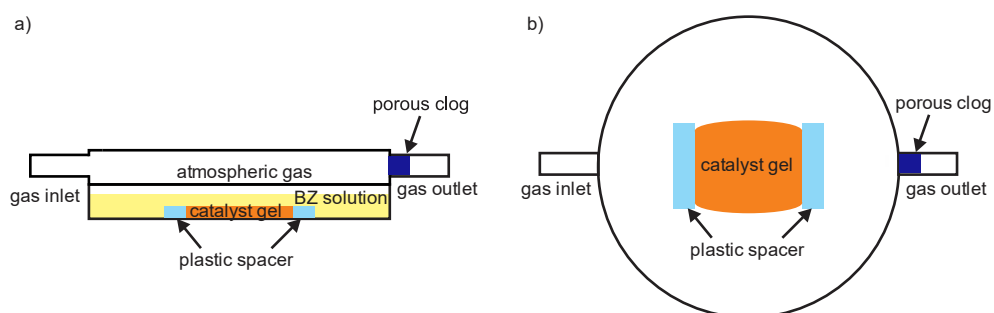


Figure S1: Schematic diagram of the reaction chamber. (a) side view, (b) top view.

ESI 2: Two-dimensional Fourier transform in the spatial domain

Two-dimension Fourier transform (2D-FT) in the spatial domain is a transformation of a periodic pattern from a spatial domain (in a unit of mm) to a corresponding frequency or wavenumber domain (in a unit of mm^{-1}). For an image of size $N \times N$ pixel², the 2D-FT is given by^{1,2}:

$$F(v_x, v_y) = \sum_{x=0}^{N-1} \sum_{y=0}^{N-1} f(x, y) e^{-i2\pi \left(\frac{xv_x}{N} + \frac{yv_y}{N} \right)},$$

where $i = \sqrt{-1}$. $f(x, y)$ is the grey level in the spatial domain and $F(v_x, v_y)$ is the Fourier component in each point. v_x and v_y are the wavenumbers corresponding with x and y position in the spatial domain. In the 2D-FT spectra, $F(0, 0)$ is shifted from the bottom left to the center of the 2D-FT spectrum. Since $F(v_x, v_y)$ is a complex number, therefore the absolute of $F(v_x, v_y)^2$ is used to create a power spectrum (intensity). Normally, the size of the spatial domain (601 pixel \times 601 pixel or 14.3 mm \times 14.3 mm for this work) was the same as the size of the 2D-FT spectrum. However, in this work the 2D-FT spectra were zoomed in six times because all of the patterns have a low wavenumbers (range from -50 to $+50$ pixels or from -3.5 to $+3.5$ mm^{-1}). The 2D-FT spectra were calculated by using a package in a computer programming language used for data analysis, called Interactive Data Language (IDL).

References

1. D. Ballard, C. Brown, Computer Vision, Prentice-Hall, New York, 1982, pp. 24 – 30.
2. R. Gonzales, R. Woods, Digital Image Processing, 3rd edition, Addison-Wesley Publishing Company, New Jersey, 1992, pp. 81 – 125.

ESI 3: Wave patterns observed in the aqueous and gel phases separately

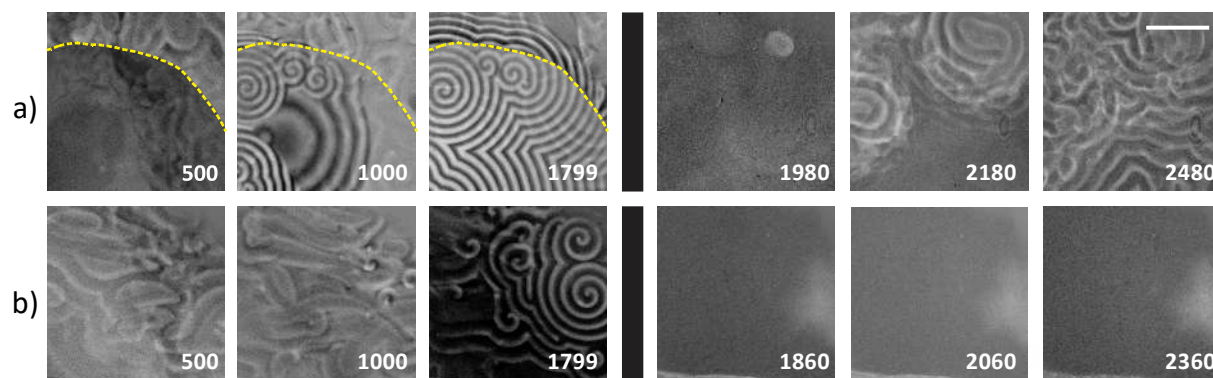


Figure S2: Regular wave patterns observed in the aqueous and gel phases separately, to confirm that the regular pattern occurs in the aqueous phase only, not in the catalyst gel. The CHD-BZ solution and the catalyst gel were separated after the time 1800 s, during the regular state for both experiments, to follow the wave dynamics in aqueous (a) and gel (b) phases after the separation. The black rectangles show the duration of the separation. The area above the yellow dashed line in the pattern (a) is no-gel area and below the dashed line is gel area. Scale bar: 5.0 mm.

The experiments were carried out by starting the reaction normally. Before the onset of the instability at 1800 s, the CHD-BZ aqueous solution was pouring out from the catalyst gel to another chamber (Petri dish). The pattern in the aqueous phase (Fig. S2a, 1980 – 2480 s) occurs in chamber without gel, the remaining gel was thrown away. The pattern in the gel (Fig. S2b, 1860 – 2360 s) was observed on the gel after the CHD-BZ aqueous solution was pouring out.

After the CHD-BZ solution was separated from the catalyst gel, there was no pattern in the catalyst gel (Fig. S2b, 1860–2360 s), but some complex waves with small wavelength can be observed in the CHD-BZ aqueous solution (Fig. S2a, 1980–2480 s). This result indicates that the initial and regular patterns at the beginning of the reaction occur in the aqueous phase.

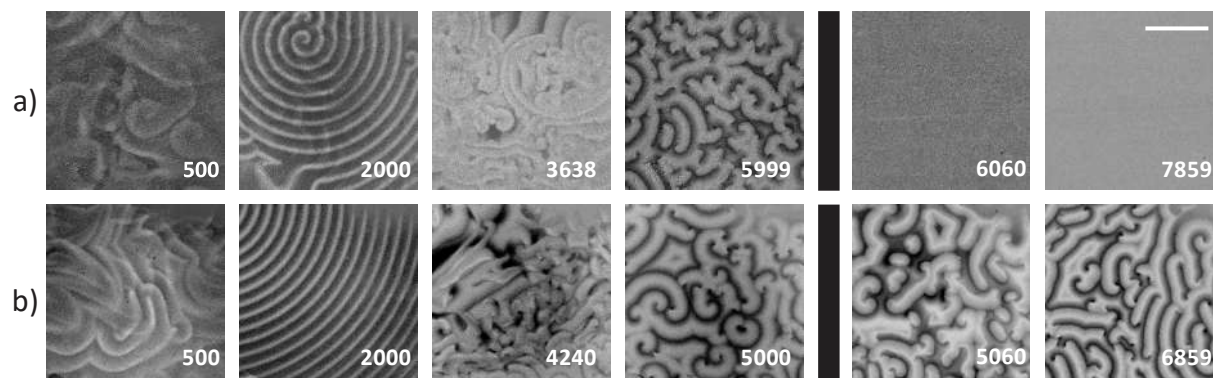


Figure S3: Turbulent wave patterns observed in the aqueous and gel phase separately, to confirm that the turbulent pattern occurs in the catalyst gel only, not in the aqueous phase. The CHD-BZ solution and the catalyst gel were separated after the time (a) 6000 s and (b) 5001 s, during the turbulent state for both experiments, to follow the wave dynamics in aqueous (a) and gel (b) phases after the separation. The black rectangles show the duration of the separation. Scale bar: 5.0 mm.

As the same method explained earlier, the experiments were carried out by starting the reaction normally and then the CHD-BZ aqueous solution was poured out after the starting of the turbulence into another chamber. The pattern in the aqueous solution (Fig. S3a, 6060 – 7859 s) was observed in the solution without gel, while the gel was neglected. The pattern in the gel (Fig. S3b, 5060 – 6859 s) was observed in the gel after the CHD-BZ solution was pouring out.

After the separation, the turbulent pattern continued to propagate in the gel phase (Fig. S3b, 5060–6859 s), while there was no pattern in the aqueous phase (Fig. S3a, 6060–7859 s). It suggests that the turbulent pattern occurs in the gel phase, not in the aqueous phase. At time 5060 s of Fig. S3b, the wave-fronts are blurring because the separation of the solution make a gradient of chemicals above the gel. Moreover, the waves do not continue with the waves before separation at 5000 s (Fig. S3b). It is because the position of chamber was changed after separation.

ESI 4: The concentrations of $\text{Ru}(\text{bpy})_3^{2+}$ releasing out of the catalyst gel phase

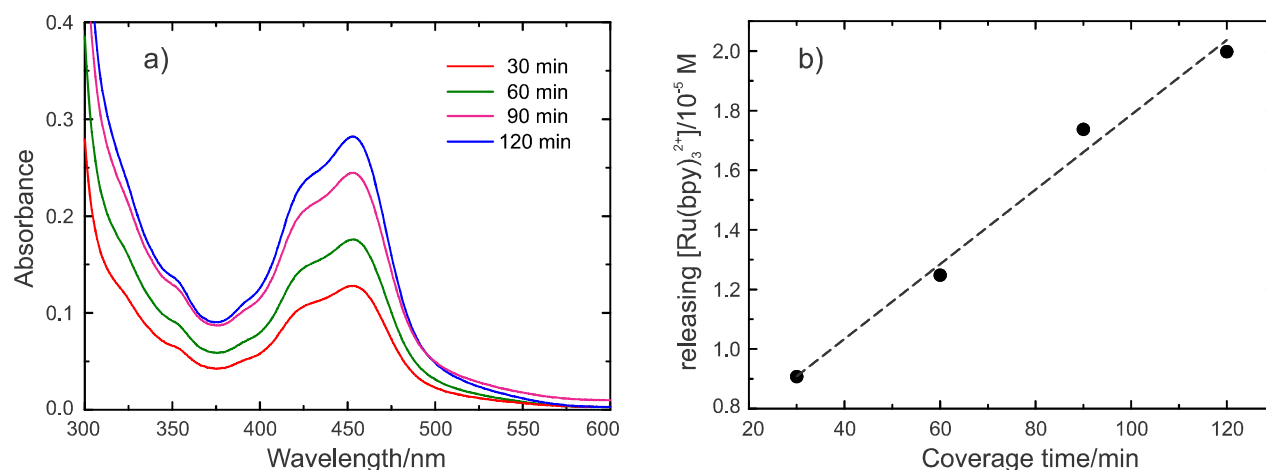


Figure S4: (a) Absorption spectra of the acid solution covering on the gel for 30 (red), 60 (green), 90 (pink), and 120 (blue) min. (b) The concentrations of $\text{Ru}(\text{bpy})_3\text{SO}_4$ released from the gel phase calculated from the absorbance in (a) at 460 nm as a function of the coverage time. The catalyst gel was covered with the acid solution (the same concentration as the acid in the CHD-BZ solution, $[\text{H}^+] = 0.39 \text{ M}$). $\epsilon_{\text{Ru(II)}} = 13400 \text{ M}^{-1}\text{cm}^{-1}$ at 460 nm.

A question arises how can the initial and regular patterns be observed (see Fig. 5) when the CHD-BZ solution consists of clear solutions: sodium bromate, CHD, sulfuric acid, and sodium bromide? Our hypothesis is that the patterns can be observed in the aqueous phase because there is a small amount of the catalyst released from the catalyst gel. The result in Fig. S4b shows that the concentrations of the released catalyst from the gel linearly increases with the increasing coverage time. The average time duration from the evaporation of bromine gas before the pattern was captured to the regular patterns was approximately 77 min or 4600 s (evaporation of Br_2 : 1800 s + initial pattern: 1500 s + regular pattern: 1300 s) corresponding with the concentration of $1.53 \times 10^{-5} \text{ M}$ of the released catalyst. According to the work by Kurin-Csörgei *et al.*¹, if the concentration of ferroin is less than $5 \times 10^{-5} \text{ M}$, then ferroin can be considered to be only an indicator of the reaction. Likewise, $\text{Ru}(\text{bpy})_3^{2+}$ was used instead ferroin in our previous work² and the results showed that at about $1.0 \times 10^{-5} \text{ M}$, $\text{Ru}(\text{bpy})_3^{2+}$ an indicator. Therefore, in this work, $\text{Ru}(\text{bpy})_3^{2+}$ in aqueous phase is also assumed to play the role of an indicator for observing the pattern in the initial and regular states.

References

1. K. Kurin-Csörgei, A. M. Zhabotinsky, M. Orbán, and I. R. Epstein, *J. Phys. Chem.* 1996, **100**, 5393-5397.
2. S. Anupong and O. Kheowan, *Pure and Applied Chemistry International Conference 2015 (PACCON2015)*, Bangkok, 2015, pp. 308-311.

ESI 5: The variations of the thickness of aqueous and gel phases

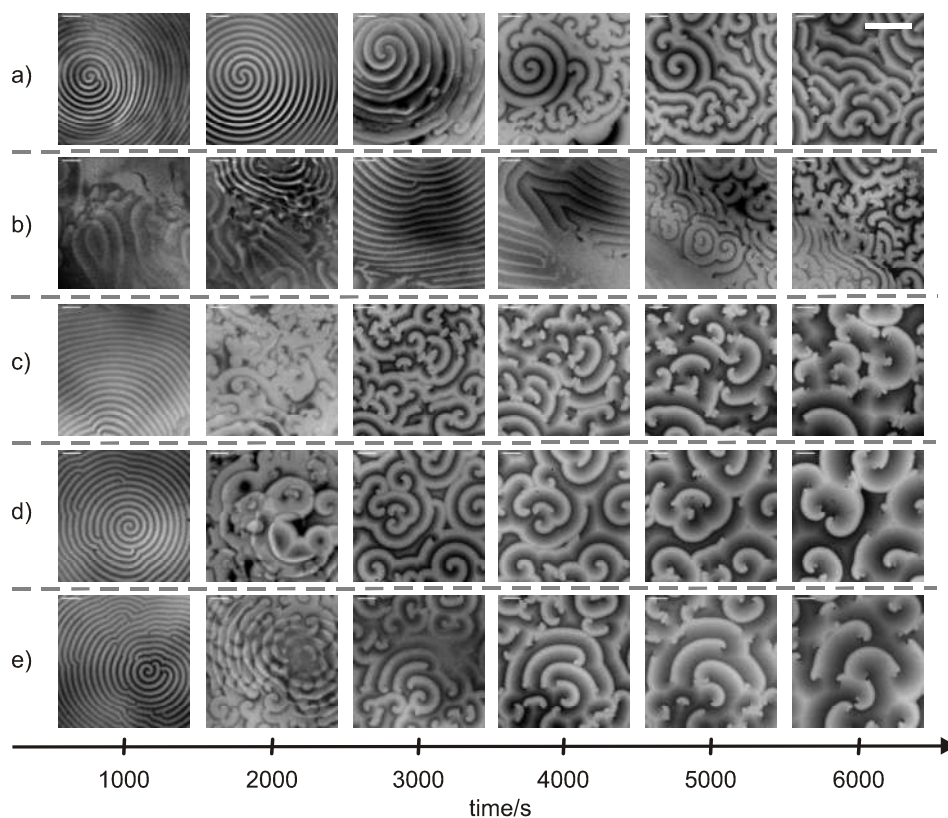


Figure S5: Wave patterns in the CHD-BZ reaction with the variation of solution thicknesses: (a) 1.94 ± 0.08 , (b) 2.32 ± 0.04 , (c) 3.25 ± 0.09 , (d) 3.43 ± 0.05 , and (e) 3.79 ± 0.02 mm. The x-axis represents time when the snapshots were captured. Scale bar: 5.0 mm.

The snapshots of wave pattern were observed in five different thicknesses of solution layer, those was 1.94 ± 0.08 , 2.32 ± 0.04 , 3.25 ± 0.09 , 3.43 ± 0.05 , and 3.79 ± 0.02 mm, while the thickness of gel layer was kept constant at 0.27 ± 0.09 mm. The thickness of gel layer did not affect the scenario of four states (initial, regular, transient, and turbulent states) for all the variation of solution thickness. Increasing of the solution thickness make the instability occurs sooner.

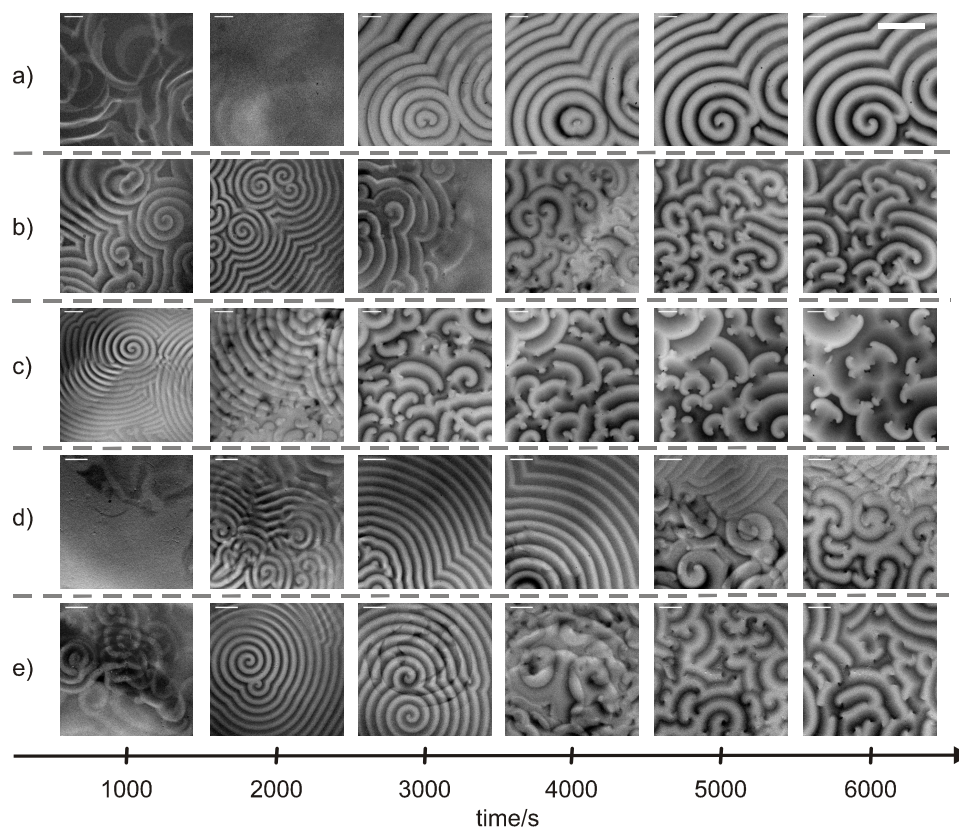


Figure S6: Wave patterns in the CHD-BZ reaction with the variation of gel thicknesses: (a) 0.16 ± 0.09 , (b) 0.27 ± 0.09 , (c) 0.32 ± 0.08 , (d) 0.44 ± 0.08 , and (e) 0.51 ± 0.06 mm. The x-axis represents time when the snapshots were captured. Scale bar: 5.0 mm.

The snapshots of wave pattern were observed in five different thicknesses of gel layer, those was 0.16 ± 0.09 , 0.27 ± 0.09 , 0.32 ± 0.04 , 0.44 ± 0.08 , and 0.51 ± 0.06 mm, while the thickness of solution layer was kept constant at 2.32 ± 0.04 mm. With the very thin thickness, there was no wave stability as the transient and turbulent states. The thickness of gel layer did not affect the scenario of four states (initial, regular, transient, and turbulent states) for higher thickness of gel at 0.27 ± 0.09 , 0.32 ± 0.08 , 0.44 ± 0.08 , and 0.51 ± 0.06 mm.

ESI 6: The initial concentrations of 1,4-cyclohexanedione

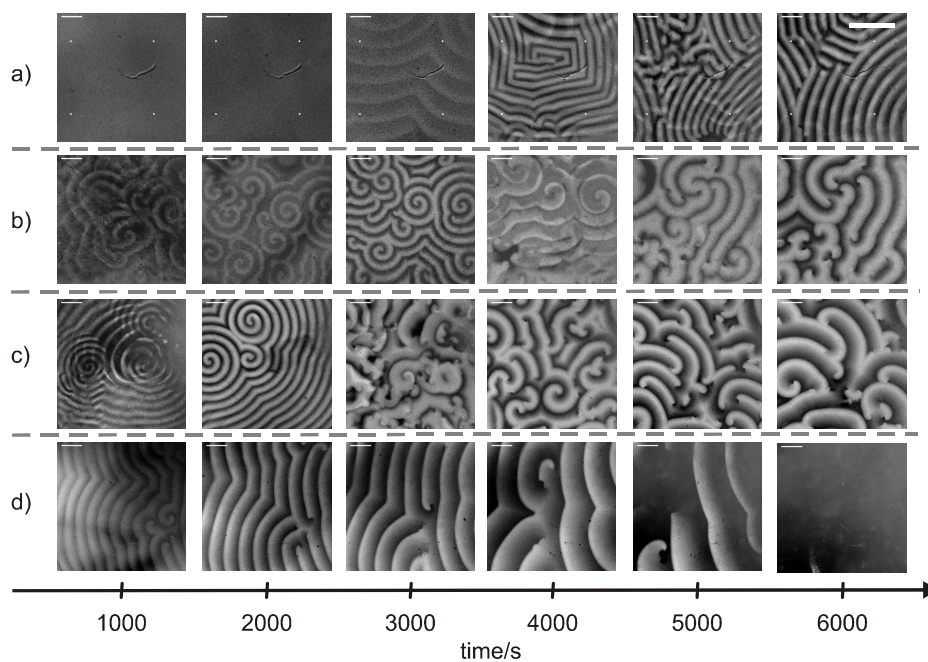


Figure S7: Wave patterns in the CHD-BZ reaction with the variation of the initial concentrations of 1,4-cyclohexanedione (CHD): (a) 0.09, (b) 0.14, (c) 0.19, and (d) 0.24 M. The x-axis represents time when the snapshots were captured. Scale bar: 5.0 mm.

The initial concentrations of 1,4-cyclohexanedione (CHD) was varied as 0.09, 0.14, 0.19, and 0.24 M. There was no instability of wave pattern at too small, 0.09 M, or too large, 0.24 M, of initial concentrations of CHD. At 0.14 and 0.19 M of the initial concentrations of CHD, the scenario of four states of pattern occurs as shown.